

An ISAR-SAR based Localization Method using Passive UHF RFID System with Mobile Robotic Platform

Zheng Liu
Centre for Photonic Systems,
Electrical Division, Department
of Engineering
University of Cambridge
Cambridge, U.K.
zl390@cam.ac.uk

Zhe Fu
Centre for Photonic Systems,
Electrical Division, Department
of Engineering
University of Cambridge
Cambridge, U.K.
zf233@cam.ac.uk

Tongyun Li
Centre for Photonic Systems,
Electrical Division, Department
of Engineering
University of Cambridge
Cambridge, U.K.
tl299@cam.ac.uk

Ian White
University of Bath
Bath, U.K.
ihw3@cam.ac.uk

Richard Penty
Centre for Photonic Systems,
Electrical Division, Department
of Engineering
University of Cambridge
Cambridge, U.K.
rvp11@cam.ac.uk

Michael Crisp
Centre for Photonic Systems,
Electrical Division, Department
of Engineering
University of Cambridge
Cambridge, U.K.
mjc87@cam.ac.uk

Abstract—A novel RFID synthetic aperture radar (SAR) based localization method using an antenna trajectory estimated using known reference tags of known location is proposed and demonstrated to find the location of target tags whose location is not known. A robot with an integrated RFID reader and antenna is used to obtain phase measurements of both the reference and target tags in an indoor environment. The trajectory of the moving RFID antenna is estimated using an Inverse SAR (ISAR) sensing algorithm. The trajectory is then combined with the phase measurements of the target tags to compute their location using a

they exist within the inventory. With such an approach, the time and cost spent searching for objects which is generally performed by humans would be significantly reduced [4,5].

Phase-based localization is a method popular as it is more robust in complex indoor environments compared to localization solutions adopting received signal strength indicator (RSSI)-based and angle of arrival (AoA)-based methods. Many different phase-based methods have been proposed to locate target objects [6-19]. Among them, the Synthetic Aperture Radar (SAR) which exploits movement of the reader antenna, is a promising solution to perform 2D and 3D localization in an indoor environment since little radio hardware is required compared to other methods [7, 8]

The various types of mobile platform have been used to generate the required movement of the reader antenna including a robotic arm [11], a robot [6-9, 19,20] or a drone [12, 13, 18]. In all cases, the trajectory of the moving RFID antenna is prerequisite to find target tag location. Several methods determine the antenna trajectory using an optical system [7, 8] or a combination of cameras and light detection and ranging (LiDAR) to perform a simultaneous localization and mapping (SLAM) algorithm [9, 19-21]. Others require the mobile platform to be equipped with a global positioning system (GPS) sensor for outdoor scenarios [12, 13, 18]. In [12], GPS based outdoor RFID localization is demonstrated using SAR. It shows 2.3 cm and -4.4 cm error at x and y axis respectively. Phase relock provides another method of localization which focusses on unwrapping and reconstructing the phase measurements [20]. Here a combination of sensors is used to perform SLAM resulting in a mean error of about 17 cm in x and y planes is achieved. In [21], a phase fingerprinting localization method is presented. The mean error is 15-22 cm and the reader antenna location is estimated by SLAM with various sensors. However,

978-1-7281-5576-0/20/\$31.00 ©2020 IEEE

conventional SAR algorithm. The performance is compared to target tags located by SAR where the antenna trajectory is measured by LiDAR. Experimental results show similar performance (15cm mean absolute error) using both LiDAR-SAR and ISAR-SAR algorithms. Compared to previous SAR based systems, the ISAR-SAR based RFID system is a cost-effective solution which is more commercially attractive for inventory tracking applications.

Keywords—RFID; SAR; ISAR; Localization; reference tags

I. INTRODUCTION

Over the past decade, passive UHF-RFID (Radio Frequency Identification) technology has attracted increasing interest for low-cost and easy-deployable solutions to provide identification objects enabling real time inventory in various scenarios such as warehouses, factories and stores [1]. There is also an increasing demand to provide accurate location information about RFID-tagged materials and products to augment the inventory information, further improving decision making [2, 3]. For example, where automated robots are to be used to fetch desired material, they must know where items are located, not just that

all these solutions are either using expensive infrastructures or sensors. A cost-effective solution is desirable for reducing the capital expenditure (CAPEX) and operational expenditure (OPEX) of the system.

In this paper, a low cost ISAR-SAR localization method is proposed and demonstrated for the first time. Instead of using expensive and bulky equipment such as LiDAR [9, 19-21] or camera-based sensor network [7, 8], the antenna trajectory is estimated using a group of very low-cost passive RFID reference tags with known locations which can be placed on physically meaningful locations (e.g. shelf bays, loading areas) so that the implementation cost could be reduced significantly. As low-cost robots will not accurately follow a specified path which is well known to cause errors in the movement, the ISAR-SAR system continuously tracks the movement of the robot and then determines the target unknown tag locations using a novel ISAR-SAR loop which is the core part of the method which will be explained more detailed later. Although it is not the focus of this study, we believe our approach is also a first step toward the implementation of a simultaneous location and mapping (SLAM) based purely on RFID.

In order to analyse the performance, results are compared with a LiDAR based system. Both the LiDAR measured trajectory and the estimated ISAR trajectory are used to locate target unknown tags using the SAR method as an evaluation of the system performance.

The remainder of the paper is organized as follows. In Section II, the RFID robotic system is introduced. The ISAR-SAR localization algorithm is explained in Section III which is followed by experiment setup and results in Section IV. Conclusion is presented in Section V.

II. SYSTEM DESIGN AND IMPLEMENTATION

As shown in Fig. 2.1, this ISAR-SAR based RFID robot mainly consists of a Turtlebot3 waffle pi robot [23], an Impinj Speedway RFID reader [22] with antenna mounted on a wooden pole attached to the robot, and two Raspberry Pi controller boards [24]. The RFID reader interrogates the tags, providing both the EPC and phase information. The data is collected for offline processing. The Turtlebot3 Waffle Pi is remotely controlled to move along a straight line. LiDAR data can be simultaneously collected and timestamped to the RFID data. (See Fig. 2.2).

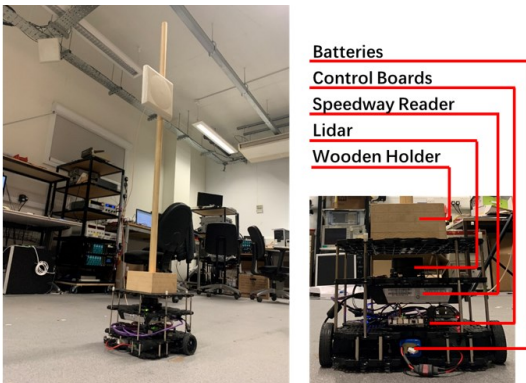


Fig. 2.1. New Designed RFID Robot

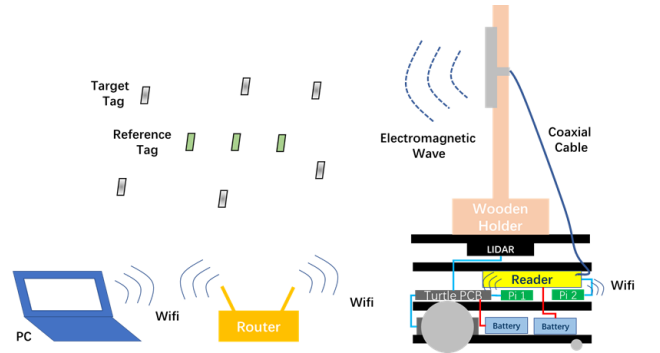


Fig. 2.2. ISAR-SAR system

III. LOCALIZATION ALGORITHM

Fig. 3.1 shows a diagram of ISAR-SAR processing. After obtaining phase information, ISAR algorithm is applied to estimate the trajectory of the RFID antenna. When the best fitting trajectory has been estimated, RFID SAR algorithm is then used to locate target tags. Since the algorithm for antenna trajectory tracking exploits the similar idea to SAR, the SAR method will be explained first, followed by the ISAR algorithm for antenna trajectory tracking and then the ISAR-SAR algorithm. The novel ISAR-SAR loop, which is the core part of the ISAR-SAR algorithm, consists of two parts. The first part is to estimate the trajectory by using ISAR algorithm, and the second part is to calculate the location of reference tag by using SAR algorithm. The real location and estimated location of reference tags will be compared as an index of accuracy and accordingly the loop could adjust its parameters to achieve a better fitting trajectory and hence achieve a higher localization accuracy. The ISAR-SAR loop will also eliminate the variation in speed and bearing during measurement so that the accuracy of target tags localization could be increased.

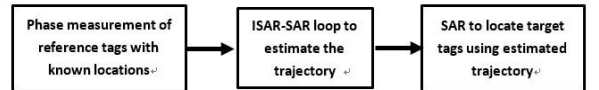


Fig. 3.1. The diagram of ISAR-SAR method

A. SAR Algorithm

The SAR localization method can be divided into two main steps. Phase information of backscattered signals from RFID tags is received by the mobile reader with a known trajectory. A probability heatmap or a holograph is calculated by a spatial ambiguity function based on received phase values. The position of the target is estimated as the location with the highest probability.

At time t , location of the reader antenna can be written as

$$\mathbf{q}_t = [x_t, y_t] \quad (1)$$

so the trajectory can be written as a vector of locations

$$\mathbf{Q} = [q_1, \dots, q_t, \dots, q_{T_1}]^T \quad (2)$$

Where T is the transpose operator and each element represents a timestep at which observation of the tag phase are taken.

The potential locations of the tag can be written as a vector by applying a grid to the area with the k -th hypothetical location of the n -th tag:

$$\mathbf{b}'_{nk} = [x'_{nk}, y'_{nk}] \quad (3)$$

The distance between each potential location and the reader antenna is then calculated by the following equation

$$d_{t,nk} = \|\mathbf{q}_t - \mathbf{b}'_{nk}\| \quad (4)$$

Where $\|\cdot\|$ is the norm operator of the distance vector.

The phase which would be recorded for a tag at each location can then be calculated:

$$\phi'_{t,nk} = \left(\phi_0 + \frac{4\pi d_{t,nk}}{\lambda} \right) \text{mod } 2\pi \quad (5)$$

Where ϕ_0 is the phase shift caused by equipment such as wires

The relative, measured, received phase backscattered by the n -th tag is

$$\Delta\phi_{t,n} = \phi_{t,n} - \phi_{1,n} \quad (6)$$

So, the sequence of relative received phases over time T could be written as

$$\Delta\Phi_n = [0, \Delta\phi_{2,n}, \dots, \Delta\phi_{t,n}, \dots, \Delta\phi_{T,n}]^T \quad (7)$$

The relative calculated phase is of each potential tag position is

$$\Delta\phi'_{t,nk} = \phi'_{t,nk} - \phi'_{1,nk} \quad (8)$$

Hence, the sequence of relative calculated phases can be expressed as

$$\Delta\Phi'_{nk} = [0, \Delta\phi'_{2,nk}, \dots, \Delta\phi'_{t,nk}, \dots, \Delta\phi'_{T,nk}]^T \quad (9)$$

The matching function is defined as

$$\mathbf{C}_n = \exp(-j(\Delta\Phi'_{nk} - \Delta\Phi_n)) \quad (10)$$

is a measure of the difference between the expected and recorded phase for each time step. The use of the complex field resolves the wrapping problem with the phase angles recognizing that the phase shift between $\Delta\phi$ and $2\pi - \Delta\phi$, is $2\Delta\phi$ rather than $2\pi - 2\Delta\phi$

The probability can be expressed as sum of the matching function

$$P_n = \left| \sum_{t=1}^T \mathbf{C}_n \right| \quad (11)$$

The location of the n -th tag would be the location with the highest probability

$$\mathbf{b}_n = \underset{\mathbf{b}'_{nk}}{\operatorname{argmax}} P_n \quad (12)$$

B. ISAR Algorithm for Antenna Trajectory Tracking

The inverse-SAR (ISAR) algorithm exploits a similar idea to that used in the SAR method. Instead of a moving platform of known trajectory to find the locations of a number of static tags of unknown location, a number of passive RFID tags of known locations are used to find the moving antenna trajectory.

At time $t-1$, the location of the reader antenna is

$$\mathbf{a}_{t-1} = [x_{t-1}, y_{t-1}] \quad (13)$$

The antenna then moves according to the j -th hypothetical step

$$\mathbf{v}_{t,j} = [l \cos \theta, l \sin \theta] \quad (14)$$

Where l is the distance moved which belongs to the range $L = [l_{min}, l_{max}]$ hence $l \in (l_{min}, l_{max})$, θ is the angle of direction which belongs to the range $\mathcal{D} = [\theta_{min}, \theta_{max}]$ hence $\theta \in (\theta_{min}, \theta_{max})$,

This results in a new hypothetical location at time t

$$\mathbf{a}'_{t,j} = \mathbf{a}_{t-1} + \mathbf{v}_{t,j} \quad (15)$$

The known location of m -th reference tag is

$$\mathbf{b}_m = [x_m, y_m] \quad (16)$$

So the distance between the antenna and tag at time t is

$$d_{t,j,m} = \|\mathbf{a}'_{t,j} - \mathbf{b}_m\| \quad (17)$$

Where $\|\cdot\|$ is the norm operator of the distance vector.

At time t , relative received phase backscattered by the m -th reference tag is

$$\Delta\phi_{t,m} = \phi_{t,m} - \phi_{1,m} \quad (18)$$

So the relative received phase of M reference tags can be written as

$$\Delta\Phi_t = [\Delta\phi_{t,1}, \dots, \Delta\phi_{t,m}, \dots, \Delta\phi_{t,M}]^T \quad (19)$$

For each hypothetical step, the expected calculated phase is given by

$$\phi'_{t,j,m} = \left(\phi_0 + \frac{4\pi d_{t,j,m}}{\lambda} \right) \text{mod } 2\pi \quad (20)$$

Where ϕ_0 is the phase shift caused by equipment such as wires

So the relative expected phase is

$$\Delta\phi'_{t,j,m} = \phi'_{t,j,m} - \phi'_{1,j,m} \quad (21)$$

Again, this can be written in vector form to account for M reference tags

$$\Delta\Phi'_{t,j} = [\Delta\phi'_{t,j,1}, \dots, \Delta\phi'_{t,j,m}, \dots, \Delta\phi'_{t,j,M}]^T \quad (22)$$

The matching function defined as

$$\mathbf{C}_{t,j} = \exp(-j(\Delta\Phi'_{t,j} - \Delta\Phi_t)) \quad (23)$$

is a measure of the difference between the expected and recorded phase for each step. The use of the complex field resolves the wrapping problem with the phase angles recognizing that the phase shift between $\Delta\phi$ and $2\pi - \Delta\phi$, is $2\Delta\phi$ rather than $2\pi - 2\Delta\phi$

The probability that each hypothetical step is correct can be calculated as sum of the result of the matching function

$$P_{t,j} = \left| \sum_{m=1}^M \mathbf{C}_{t,j} \right| \quad (24)$$

The maximum likelihood estimated location would be

$$\mathbf{a}_t = \underset{\mathbf{a}_{t,j}}{\operatorname{argmax}} P_{t,j} \quad (25)$$

And finally, a trajectory is estimated as

$$\mathbf{A} = [\mathbf{a}_1, \dots, \mathbf{a}_t, \dots, \mathbf{a}_T] \quad (26)$$

C. ISAR-SAR

After obtaining a trajectory of the antenna, the SAR algorithm is used to calculate the location of the reference tags as an accuracy check. By varying the parameters of ISAR algorithm such as the range of the length of the step L or even the range of the angle of direction ϑ , a different trajectory can be calculated resulting in different errors in the know tag locations. The localization error is compared with the expected localization error E . If it is larger than E , the trajectory will be estimated again with different parameters, which corresponds to the loop part of the process, as described in the flowchart as shown in Fig. 3.2. If there is no result smaller than E is found for a long running time, the E could be increased. By comparing the localization errors, the final trajectory would be the best fitting trajectory and will be used to locate target tags using the SAR method described in part A.

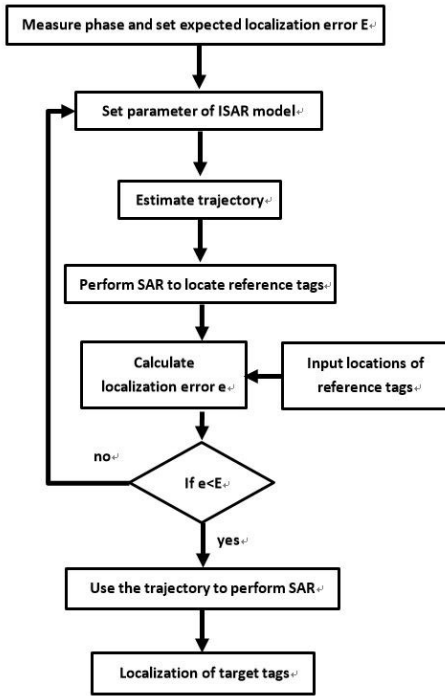


Fig. 3.2. The flow chart of ISAR-SAR method

IV. RESULTS AND DISCUSSION

An experiment was carried out using two rows of reference tags (black circles) and one row of target tags (blue crosses) as shown in Fig. 4.1(a) in an indoor environment (Fig. 4.1(b)). The antenna follows an intended trajectory shown by the blue line in Fig. 4.1(a). The first row of reference tags was placed 1.2 m away from the antenna and the second row of reference tags was placed 2 m away. Target tags were placed in the middle of two rows of reference tags. The distance between the rows of tags and tags within rows is 0.4 m. The first tag of the

first row was placed at (0.2, 1.2) and the first tag of the third row was placed at (0.4, 2.0) while the first tag of the target tags was at (0.3, 1.6).

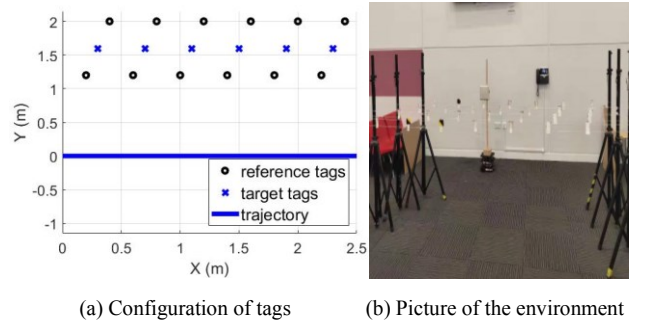


Fig. 4.1. Experiment setup

Table I shows the results of ISAR process. When l_{min}/l_{max} is changed, the estimated trajectory varies. As a result, the localization accuracy of reference tags varies. It can be seen that the best parameter would be 3.5/5.0 as it has the smallest MAE (17.49 cm) of reference tags.

TABLE I. RESULTS OF ISAR PROCESS

The MAE of localization of reference tags (cm)								
l_{min}	l_{max}	MAE	l_{min}	l_{max}	MAE	l_{min}	l_{max}	MAE
1.5	5.0	45.17	1.5	5.5	26.07	1.5	6.0	38.22
2.0	5.0	38.03	2.0	5.5	19.94	2.0	6.0	53.17
2.5	5.0	27.36	2.5	5.5	24.56	2.5	6.0	71.23
3.0	5.0	22.48	3.0	5.5	33.92	3.0	6.0	86.17
3.5	5.0	17.49	3.5	5.5	48.04	3.5	6.0	97.49
4.0	5.0	23.06	4.0	5.5	63.17	4.0	6.0	107.78

Fig. 4.2 shows measured and ISAR calculated trajectories. The two trajectories are very close to each other. Fig. 4.3 is a zoom-in view of Fig. 4.2 and shows more details of two trajectories. Blue circles represent sample points of the trajectory by LiDAR sensor and the red cross is the result of the ISAR method. The dashed lines show the corresponding relationship between two trajectories lining points corresponding to the same time step, so they represent the error vectors. The difference between the trajectories is of the order of a centimeter

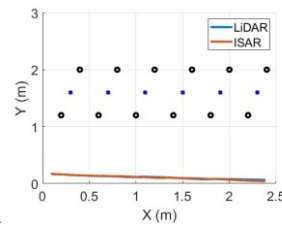


Fig. 4.2. Trajectory results of one of the experiments

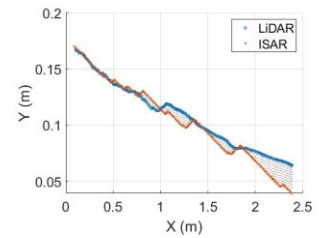


Fig. 4.3. Comparison of sample points between LiDAR trajectory and ISAR trajectory

Fig. 4.4 and Fig. 4.5 show both the error along x-axis and y-axis between the trajectory measured by LiDAR sensor and the trajectory estimated by ISAR.

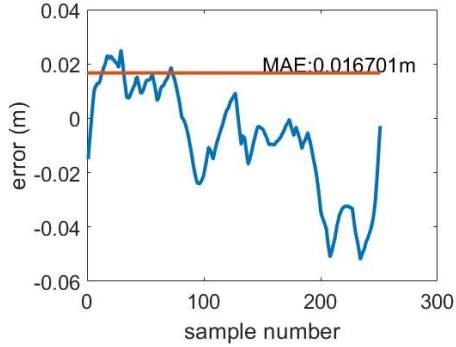


Fig. 4.4. Errors and MAE between ISAR trajectory and LiDAR trajectory along x-axis

Fig. 4.4 shows the error along x-axis. Positive value means the estimated location leads the measured location while negative value means the estimated location lags the measured location. From Fig. 3.4, although at the most of time the estimated location lags the measured location, the error along x-axis is small which is smaller than 5 cm. The mean absolute error (MAE) is about 2 cm as shown by the red line.

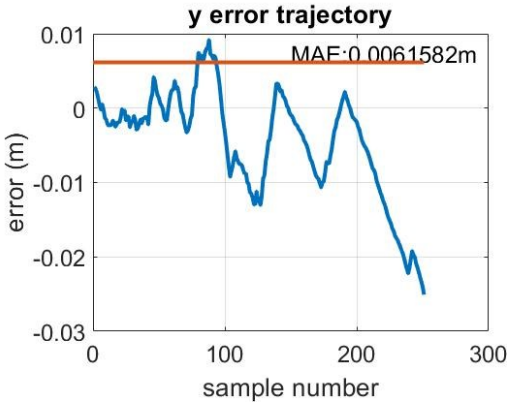


Fig. 4.5. Errors and MAE between ISAR trajectory and LiDAR trajectory along y-axis

Fig. 4.5 depicts the error along y-axis. A positive value means the estimated location is at the left side of the measured location along the moving direction while negative value means the estimated location is at the right of the measure location. The y-axis error is smaller than 2 cm and the mean absolute error is around 0.6 cm which is shown by the red line. Table I lists results of 10 tests.

TABLE II. DIFFERENCE BETWEEN TRAJECTORY MEASURED BY LIDAR AND ESTIMATED BY ISAR

Test	MAE (cm)	
	x-axis	y-axis
1	3.21	4.85
2	10.67	2.90
3	2.44	1.18

4	3.00	0.81
5	1.11	4.01
6	3.56	1.36
7	2.14	1.26
8	1.14	3.67
9	1.67	0.62
10	4.60	0.93
Mean	3.35	2.16

Table II shows the error along x-axis and y-axis. The mean of MAE of ten tests along x-axis and y-axis is around 3 cm and 2 cm respectively. As shown in the Table, except Test 2, the MAE along x-axis of other tests are smaller than 5 cm and the MAE along y-axis of ten tests are within 5 cm which is similar to the accuracy of the LiDAR. The accuracy of the LiDAR is ± 15 mm within 500 mm and $\pm 5.0\%$ when the distance is 500~3500 mm [25], so the recorded differences are within the error bounds of the LiDAR itself.

After obtaining the estimated trajectory, SAR method is carried out to locate target tags. Both the trajectory measured by LiDAR and the trajectory estimated by previous steps are used to perform the SAR method for localization of target tags. Results are shown in Fig. 4.6.

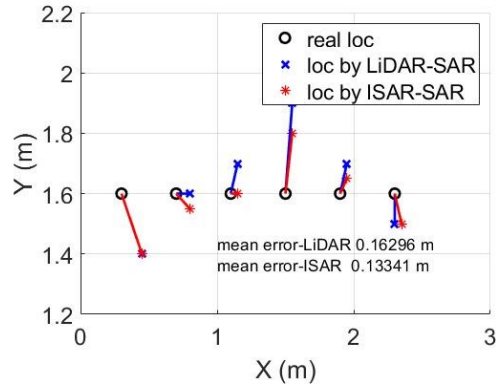


Fig. 4.6. Localization results of target tags of one of experiments

In Fig. 4.6, black circle shows the actual location of target tags, blue crosses represent the estimated location using the LiDAR trajectory while the red stars show the estimated location using the trajectory estimated by ISAR. Fig. 4.6 shows that two trajectories provide similar localization accuracy. The mean error of localization by using LiDAR trajectory is about 16 cm while that of the ISAR trajectory is around 13 cm. 10 tests have been carried out and mean localization error as well as the mean localization error in percentage with respect to the minimum reader to tag range (1.6 m) have been summarized in Table III. The mean localization error of 10 tests by using LiDAR trajectory is 15 cm while ISAR trajectory provides 15 cm accuracy which is at the same level. It is interesting to note that the errors are generally consistent between the LiDAR and SAR, we believe this is because the largest source of error is multipath propagation which will be the same in both cases.

TABLE III. MEAN LOCALIZATION ERROR OF 10 TESTS BY SAR WITH TWO TRAJECTORIES

Test	LiDAR (cm)	LiDAR	ISAR (cm)	ISAR
1	16.83	11%	19.05	12%
2	14.21	9%	13.24	8%
3	14.63	9%	15.89	10%
4	15.69	10%	15.02	9%
5	13.96	9%	14.46	9%
6	16.57	10%	21.41	13%
7	12.72	8%	12.70	8%
8	13.39	8%	11.42	7%
9	16.30	10%	13.34	8%
10	16.57	10%	14.59	9%
Mean	15.09	9%	15.11	9%

V. CONCLUSION

This paper proposes an ISAR based trajectory estimation method by deploying reference tags for accurate RFID SAR localisation. Compared to conventional RFID SAR methods using additional sensors and infrastructures, low cost phase measurement from reference tags with known locations are used to estimate the moving trajectory of the robotic mobile platform. Experimental results show that the mean absolute error between the trajectory estimated by the proposed method and the trajectory measured by LiDAR are similar to within 5 cm. The estimated trajectory can provide a 15 cm localization accuracy for an unknow tag location while the accuracy using the LiDAR measured trajectory is 15 cm. This demonstration shows that the ISAR-SAR design allows a simplified architecture which is capable of proving the same level of accuracy as the LiDAR-SAR solutions for RFID localisation. Thus, it offers a more commercially attractive solution for the inventory tracking market. The work lays the foundations for SLAM using only RFID to allow localisation without reference tags (or with very few). However, the limitations of multipath and obstacles also require further investigation.

ACKNOWLEDGEMENT

The authors would like to thank Beijing Institute of Aerospace Control Devices (BIACD) for their support through the RFID system Optimization for smart manufacturing using Mobile rEader (ROME) project.

REFERENCES

- [1] K. Nur, M. Morenza-Cinos, A. Carreras, and R. Pous, "Projection of RFID-Obtained Product Information on a Retail Stores Indoor Panoramas", *IEEE Intelligent Systems*, vol. 30, no. 6, pp. 30-37, Nov.-Dec. 2015.
- [2] W. Lu, G. Q. Huang, and H. Li, "Scenarios for applying RFID technology in construction project management," in *Automation in Construction*, vol. 20, no. 2, pp. 101-106, 2011.
- [3] R. Flanagan and W. Lu, "Making informed decisions in product-service systems," in *IMEchE Conference, Knowledge and Information Management Through-Life*, Institute of Mechanical Engineers, London, 2008.
- [4] A. Alexander, S. Phillips, and G. Shaw, "Retail Innovation and Shopping Practices: Consumers' Reactions to Self-Service Retailing," in

- Environment and Planning A: Economy and Space, 40(9), 2204-2221, 2008.
- [5] J. Koch, J. Wettach, E. Bloch, and K. Berns, "Indoor localisation of humans, objects, and mobile robots with RFID infrastructure," in 7th International Conference on Hybrid Intelligent Systems, pp. 271-276, September 2007.
- [6] Li, C., Tanghe, E., Plets, D., Suanet, P., Hoebeke, J., Poorter, E., & Joseph, W. (2019). RePos: Relative Position Estimation of UHF-RFID Tags for Item-level Localization. 2019 IEEE International Conference on RFID Technology and Applications (RFID-TA), 357-361.
- [7] Bernardini, F., Motroni, P., Nepa, P., Buffi, P., Tripicchio, & Unetti, M. (2019). Particle Swarm Optimization in Multi-Antenna SAR-based Localization for UHF-RFID Tags. 2019 IEEE International Conference on RFID Technology and Applications (RFID-TA), 291-296.
- [8] A. Motroni, P. Nepa, V. Magnago, A. Buffi, B. Tellini, D. Fontanelli, and D. Macii, "SAR-Based Indoor Localization of UHF-RFID Tags via Mobile Robot", *2018 International Conference on Indoor Positioning and Indoor Navigation (IPIN)*, Nantes, 2018, pp. 1-8.
- [9] A. Motroni, P. Nepa, A. Buffi, P. Tripicchio, and M. Unetti, "RFID Tag Localization with UGV in Retail Applications", *2018 3rd International Conference on Smart and Sustainable Technologies (SpliTech)*, Split, 2018, pp. 1-5.
- [10] A. Buffi, M. R. Pino, and P. Nepa, "Experimental Validation of a SAR Based RFID Localization Technique Exploiting an Automated Handling System", *IEEE Antennas and Wireless Propagation Letters*, vol. 16, pp. 2795-2798, 2017.
- [11] R. Miesen, F. Kirsch, and M. Vossiek, "UHF RFID localization based on synthetic apertures", *IEEE Transactions on Automation Science and Engineering*, vol. 10, no. 3, pp. 807-815, Jul. 2013.
- [12] A. Buffi, A. Motroni, P. Nepa, B. Tellini, and R. Cioni, "A SAR-Based Measurement Method for Passive-Tag Positioning With a Flying UHF RFID Reader", *IEEE Transactions on Instrumentation and Measurement*, vol. 68, no. 3, pp. 845-853, March 2019.
- [13] A. Buffi and B. Tellini, "Measuring UHF-RFID Tag Position via Unmanned Aerial Vehicle in Outdoor Scenario", *2018 IEEE 4th International Forum on Research and Technology for Society and Industry (RTSI)*, Palermo, 2018, pp. 1-6.
- [14] L. Qiu, Z. Huang, N. Wirstrom and T. Voigt, "3DinSAR: Object 3D localization for indoor RFID applications", *2016 IEEE International Conference on RFID (RFID)*, Orlando, FL, 2016, pp. 1-8.
- [15] Y. Zhang, L. Xie, Y. Bu, Y. Wang, J. Wu, and S. Lu, "3-Dimensional Localization via RFID Tag Array", *2017 IEEE 14th International Conference on Mobile Ad Hoc and Sensor Systems (MASS)*, Orlando, FL, 2017, pp. 353-361.
- [16] A. Ascher, J. Lechner, S. Nosovic, P. Eschlwech, and E. Biebl, "3D localization of passive UHF RFID transponders using direction of arrival and distance estimation techniques", *2017 IEEE 2nd Advanced Information Technology, Electronic and Automation Control Conference (IAEAC)*, Chongqing, 2017, pp. 1373-1379.
- [17] G. Alvarez-Narciandi, J. Laviada, M. R. Pino, and F. Las-Heras, "3D location system based on attitude estimation with RFID technology", *2017 IEEE International Conference on RFID Technology & Application (RFID-TA)*, Warsaw, 2017, pp. 80-82.
- [18] A. Buffi, P. Nepa, and R. Cioni, "SARFID on drone: Drone-based UHF-RFID tag localization," in *2017 IEEE International Conference on RFID Technology & Application (RFID-TA)*, 2017.
- [19] Tzitzis, A., Megalou, S., Siachalou, S., Tsardoulias, E., Yioultsis, T., & Dimitriou, A. (2019). 3D Localization of RFID Tags with a Single Antenna by a Moving Robot and "Phase ReLock". 2019 IEEE International Conference on RFID Technology and Applications (RFID-TA), 273-278. Phase ReLock - Localization of RFID Tags by a Moving Robot
- [20] Tzitzis, A., Megalou, S., Siachalou, S., Yioultsis, T., Kehagias, A., Tsardoulias, E., Dimitriou, A. (2019). Phase ReLock - Localization of RFID Tags by a Moving Robot. 2019 13th European Conference on Antennas and Propagation (EuCAP), 1-5.
- [21] Siachalou, S., Megalou, S., Tzitzis, A., Tsardoulias, E., Bletsas, A., Sahalos, J., Dimitriou, A. (2019). Robotic Inventorying and Localization

- of RFID Tags, Exploiting Phase-Fingerprinting. 2019 IEEE International Conference on RFID Technology and Applications (RFID-TA), 362-367.
- [22] Impinj, Inc, “ IMPINJ SPEEDWAY READER OVERVIEW, SOFTWARE TOOLS, ACCESSORIES, AND SPECIFICATIONS”, Impinj”, Impinj Speedway R420 datasheet <https://support.impinj.com/hc/en-us/articles/202755388-Speedway-Reader-Family-Product-Brief-Datasheet>
- [23] ROBOTIS, INC., “Hardware Specifications”, Turtlebot3 Waffle Pi datasheet <http://emanual.robotis.com/docs/en/platform/turtlebot3/specifications/>
- [24] Raspberry Pi Foundation , “Raspberry Pi Compute Module 3+ Raspberry Pi Compute Module 3+ Lite”, Raspberry Pi datasheet https://www.raspberrypi.org/documentation/hardware/computemodule/datasheets/rpi_DATA_CM3plus_lp0.pdf
- [25] ROBOTIS, INC, “360 Laser Distance Sensor LDS-01 (LIDAR)”, [903-0258-000] 360 Laser Distance Sensor LDS-01 <http://www.robotis.us/360-laser-distance-sensor-lds-01-lidar/>